AIP | The Journal of Chemical Physics

# Accurate theoretical study of PSq (q = 0,+1,−1) in the gas phase

Saida Ben Yaghlane, Joseph S. Francisco, and Majdi Hochlaf

Citation: The Journal of Chemical Physics **136**, 244309 (2012); doi: 10.1063/1.4730303
View online: http://dx.doi.org/10.1063/1.4730303
View Table of Contents: http://scitation.aip.org/content/aip/journal/jcp/136/24?ver=pdfcov
Published by the AIP Publishing



# Accurate theoretical study of $PS^q$ (q = 0,+1,−1) in the gas phase

Saida Ben Yaghlane,[1] Joseph S. Francisco,[2,a)] and Majdi Hochlaf[3,a)]
[1]*Laboratoire de Spectroscopie Atomique, Moléculaire et Applications – LSAMA, Université de Tunis, Tunis, Tunisia*
[2]*Department of Chemistry and Department of Earth and Atmospheric Sciences, Purdue University, West Lafayette, Indiana 47906, USA*
[3]*Université Paris-Est, Laboratoire Modélisation et Simulation Multi Echelle, MSME UMR 8208 CNRS, 5 bd Descartes, 77454 Marne-la-Vallée, France*

(Received 4 April 2012; accepted 6 June 2012; published online 27 June 2012)

Highly correlated *ab initio* methods were used in order to generate the potential energy curves and spin-orbit couplings of electronic ground and excited states of PS and $PS^+$. We also computed those of the bound parts of the electronic states of the $PS^-$ anion. We used standard coupled cluster CCSD(T) level with augmented correlation-consistent basis sets, internally contacted multi-reference configuration interaction, and the newly developed CCSD(T)-F12 methods in connection with the explicitly correlated basis sets. Core-valence correction and scalar relativistic effects were examined. Our data consist of a set of spectroscopic parameters (equilibrium geometries, harmonic vibrational frequencies, rotational constants, spin-orbit, and spin-spin constants), adiabatic ionization energies, and electron affinities. For the low laying electronic states, our calculations are consistent with previous works whereas the high excited states present rather different shapes. Based on these new computations, the earlier ultraviolet bands of PS and $PS^+$ were reassigned. For $PS^-$ and in addition to the already known anionic three bound electronic states (i.e., $X^3\Sigma^-$, $^1\Delta$, and $1^1\Sigma^+$), our calculations show that the $^1\Sigma^-$, $^3\Sigma^+$, and the $^3\Delta$ states are energetically below their quartet parent neutral state ($a^4\Pi$). The depletion of the J = 3 component of $PS^-(^3\Delta)$ will mainly occur via weak interactions with the electron continuum wave. © *2012 American Institute of Physics*. [http://dx.doi.org/10.1063/1.4730303]

## I. INTRODUCTION

The first identification of PS molecule came from the studies of Dressler and Miescher in 1955.[1,2] These authors formed this radical via a transformer discharge and had identified two band systems of PS, one in the ultraviolet (UV) (X ← C transition) and the other one in the visible region (X ← B transition), corresponding to the emission transitions populating the ground state (GS) of this radical. Later on, the ultraviolet band was recorded again and reanalyzed by Narasimham and Balasubramanian[3,4] and then by Jenouvrier and Pascat.[5] A rough estimate of the dissociation energy and the ionization energy (IE) of PS is determined by Drowart *et al.*[6] More recently, the rotational spectra of PS up to 1 THz were recorded by Klein *et al.*[7] allowing to resolve the hyperfine structure caused by the P-atom and to derive a full set of molecular parameters including the rotational constants, the fine-structure constants, the Λ-doubling parameter, and the magnetic hyperfine constants.

No theoretical studies of the electronic spectrum of PS have been reported before the configuration interaction (MRD-CI) studies by Karna *et al.*[8] in 1988. In addition to the X, B, and C states previously known, several bound electronic excited states are predicted. These authors have also computed the electronic affinity (EA) and the IE of PS and performed an extensive basis set and configuration interaction study of the dipole moment, electric field gradient, and hyperfine parameters of the $X^2\Pi$ state of PS at the experimental equilibrium internuclear distance.[9] The ROHF, UHF, GVB studies of Moussaoui *et al.*[10] and the comparison of their results to the MRD-CI data of Karna *et al.*[8] and to the available experimental data showed that a post Hartree-Fock treatment utilizing large basis sets is mandatory for the description of this radical at spectroscopic accuracy. Klacher[11] computed the electron affinity of PS at the CAS-ACPF level of theory.

Experimental observation of the ionized forms of PS is scarce. For $PS^+$, primary experimental observation is reported in the emission spectra of Dressler and Miescher[1,2] who identified the ground and an excited state of the $PS^+$ ion. Through analysis of the UV measured band, they derived the harmonic wavenumbers of the emitting state, of the ground state and of the transition energy. Theoretically, we should mention the ROHF, UHF, GVB studies by Moussaoui *et al.*[10] and the MRD-CI computations by Karna *et al.*[12] The spectrum of $PS^-$ is known to have three bound electronic states from the theoretical work of Bruna and Grein.[13] To the best of our knowledge, there is no experimental identification of this anion.

From an astrophysical point of view, the simplest diatomic molecule formed by the association of phosphorus (P) and sulfur (S) atoms is PS. This diatomic molecule has yet to be detected, in spite of the fact that a wide variety of molecules containing either phosphorus or sulfur atoms have been detected and identified in interstellar medium

a)Authors to whom correspondence should be addressed. Electronic addresses: francisc@purdue.edu and hochlaf@univ-mlv.fr. Phone: +33 1 60 95 73 19. FAX: +33 1 60 95 73 20.

 

(ISM) by rotational and vibrational spectroscopy in the radio, microwave, or infrared regions of the spectrum. The list of molecules includes diatomics, triatomics, and even tetratomics either neutral or positively charged.[14–30] This lack of observation is related to the limited spectroscopic information available in the literature for PS and its ions, $PS^+$ and $PS^-$.

In the present paper, different *ab initio* methods are used to compute the equilibrium structure of PS and its ions, $PS^+$ and $PS^-$. This includes coupled cluster, internally contacted multi-reference configuration interaction (MRCI), and the newly developed CCSD(T)-F12 methods. For the description of P and S atoms, several basis sets are tested. The electronic excited states of PS, $PS^+$, and $PS^-$ using MRCI approach in conjunction with a large basis set is also investigated. Spin-orbit and spin-spin constants and a set of accurate spectroscopic data including equilibrium distances, harmonic, anharmonic terms, and rotational constants are reported to facilitate experimental and astrophysical observation of PS and its ions.

## II. COMPUTATIONAL METHODS

All calculations were done using the MOLPRO (Ref. 31) program suite. These calculations consist of generation of the potential energy curves (PECs) of the ground electronic states of PS, $PS^-$, and $PS^+$ using multi- and mono-configurational approaches. These calculations are done using the coupled cluster method with perturbative treatment of triple excitations ((R)CCSD(T)),[32–34] the complete active space self-consistent field (CASSCF),[35,36] followed by the internally contracted MRCI method[37,38] and the newly developed and implemented (R)CCSD(T)-F12 technique (using both F12a and F12b approximations)[39,40] (cf. Ref. 41) with the explicitly correlated basis set by Peterson and co-workers[42] in conjunction with corresponding auxiliary basis sets and density fitting functions[43–45] to treat the correlation energy of the valence electrons. In the CASSCF calculations, all valence molecular orbitals are optimized and all electrons are correlated. In the MRCI, all configurations of the CI expansion of the CASSCF wavefunctions are taken into account as a reference.

Core-valence correlation and relativistic corrections are examined as well. For the description of the S and P atoms, the following basis sets are used: aug-cc-pVXZ, aug-cc-pCVXZ (within the frozen core and within the core zero approximations for core-valence correlation), aug-cc-pVXZ-DK, and aug-cc-pV(X+d)Z for X = T,Q.[46–51] In addition, the electronic excited states of PS, $PS^-$, and $PS^+$ are examined using the CASSCF/MRCI approach with the aug-cc-pV5Z basis set.[46,47]

Finally, the potentials are incorporated into a perturbative treatment of the nuclear motion problem using the method of Cooley.[52] The spectroscopic constants discussed below were obtained using the derivatives at the minimum energy distances and standard perturbation theory.

## III. SYSTEMATIC STUDIES ON THE ELECTRONIC GROUND STATES OF PS, $PS^+$, AND $PS^-$

A systematic study of the properties of the ground electronic states of PS, $PS^+$, and $PS^-$ using mono-configurational, multi-configurational approaches are presented in Table I. The ground electronic state of PS is of $^2\Pi$ nature with a bond length of 1.896 Å at the RCCSD(T)/aug-cc-pCVQZ level of theory. Removal of an electron from the outermost orbital of PS, which is anti-bonding in nature, leads to the formation of $PS^+$ cation in the $^1\Sigma^+$ state, where the P-S bond shortens significantly (by about 0.07–0.08 Å). Addition of one electron to the outermost orbital of PS results in the formation of the bound $PS^-$ ($X^3\Sigma^-$) state, where the P-S distance increases by about 0.1 Å. This is in good agreement with previous theoretical computations on neutral and ionized PS species. This is also the case for the isovalent molecules.[53–55]

The spectroscopic data listed in Table I were obtained after generating the potential energy curves of the corresponding states and after nuclear motion treatment. For all three species, this table shows that there is convergence in the equilibrium distance as the size of the basis set increases. When we compare the P-S distances in PS, $PS^+$, and $PS^-$ computed using the aug-cc-pVXZ for X = D to 5 basis sets, one can clearly see that this distance shortens by 0.017–0.02 Å when increasing the size of the basis set, whatever the electronic structure method used (either MRCISD or (R)CCSD(T)). The harmonic wavenumbers are also increasing by 15–20 $cm^{-1}$ by increasing the size of the basis set. Nevertheless, the anharmonic terms remain roughly unchanged. The inclusion of tight-d functions leads also to the shortening of the P-S equilibrium distance. For instance, the RCCSD(T) $R_e$ distance of PS($X^2\Pi$) shortens from 1.901 Å using aug-cc-pVQZ to 1.897 Å with the aug-cc-pV(Q+d)Z. Moreover, a shortening of the $R_e$ distance is observed when there is better accounting for electron correlation: $R_e$(PS $X^2\Pi$) at MRCISD/aug-cc-pV5Z level is 1.900 Å and $R_e$(PS $X^2\Pi$) at RCCSD(T)/aug-cc-pV5Z level is 1.895 Å. It is worthwhile to note that the equilibrium distances obtained at the (R)CCSD(T)/aug-cc-pV(Q+d), (R)CCSD(T)/core 0/aug-cc-pVQZ, (R)CCSD(T)/aug-cc-pV5Z and (R)CCSD(T)-F12/VTZ-F12 levels are almost identical. Similar remarks can be drawn for the rotational constants, $B_e$ and for the harmonic wavenumbers, $\omega_e$. The anharmonic terms ($\omega_e x_e$, $\omega_e y_e$, $\alpha_e$) are less sensitive to basis set and electron correlation effects. One would compute almost similar values independent of the level of theory used for the computations.

Since it has been largely verified that the (R)CCSD(T)-F12/VTZ-F12 approach can lead to relative energies and molecular spectroscopic properties as accurate as those obtained with the more computationally demanding (R)CCSD(T)/aug-cc-pV5Z method. This is widely proved in the literature via benchmarks on different molecular systems (see, for instance, Ref. 41). Therefore, we consider our (R)CCSD(T)-F12/VTZ-F12 results as both the best estimate of and closest to experimental values for the investigated parameters. We recommend, hence, the RCCSD(T)-F12/VTZ-F12 values for direct comparison with experimental data. As an illustration, the computed spectroscopic parameters for PS ($X^2\Pi$) are compared to the experimental results of Jenouvrier and Pascat.[5] For example, the RCCSD(T)-F12/VTZ-F12 harmonic frequency, $\omega_e$ of 737.9 $cm^{-1}$, compares favorably with the experimental value of 739.5 $cm^{-1}$. The anharmonic $\omega_e x_e$ term (=2.91 $cm^{-1}$) is also quite close to their measurement

TABLE I. Equilibrium distances ($R_e$, Å), spectroscopic parameters (harmonic and anharmonic terms and rotational constants, $cm^{-1}$), and total energies ($E_h$, Hartree) for neutral and ionic PS ground states.

| Method | Basis set | $R_e$ | $\omega_e$ | $\omega_e x_e$ | $\omega_e y_e$ | $\alpha_e$ | $B_e$ | Energy |
|---|---|---|---|---|---|---|---|---|
| | | | | PS ($X^2\Pi$) | | | | |
| MRCISD | aug-cc-pVTZ | 1.918 | 715.4 | 2.98 | −0.0030 | 0.001 56 | 0.288 46 | −738.596 39 |
| | aug-cc-pVQZ | 1.906 | 727.8 | 2.97 | −0.0025 | 0.001 55 | 0.291 90 | −738.619 28 |
| | aug-cc-pV5Z | 1.900 | 732.7 | 2.95 | −0.0023 | 0.001 55 | 0.293 75 | −738.628 10 |
| RCCSD(T) | aug-cc-pVTZ | 1.913 | 725.9 | 2.83 | −0.0045 | 0.001 51 | 0.289 74 | −738.627 84 |
| | aug-cc-pVQZ | 1.901 | 739.2 | 2.87 | 0.0037 | 0.001 51 | 0.293 42 | −738.654 54 |
| | aug-cc-pV5Z | 1.895 | 744.1 | 2.80 | −0.0017 | 0.001 50 | 0.295 32 | −738.664 52 |
| | aug-cc-pV(T+d)Z | 1.905 | 731.1 | 2.88 | 0.0009 | 0.001 52 | 0.292 16 | −738.632 42 |
| | aug-cc-pV(Q+d)Z | 1.897 | 742.4 | 2.82 | −0.0032 | 0.001 51 | 0.294 78 | −738.657 32 |
| | aug-cc-pVTZ-DK | 1.905 | 731.7 | 2.81 | −0.0063 | 0.001 52 | 0.292 25 | −738.142 08 |
| | aug-cc-pVQZ-DK | 1.895 | 743.5 | 2.77 | −0.0082 | 0.001 51 | 0.295 22 | −738.157 36 |
| | aug-cc-pCVTZ | 1.906 | 730.8 | 2.84 | −0.0034 | 0.001 52 | 0.292 11 | −738.633 80 |
| | aug-cc-pCVQZ | 1.896 | 743.1 | 2.82 | −0.0049 | 0.001 51 | 0.295 10 | −738.659 01 |
| RCCSD(T)/core0 | aug-cc-pVTZ | 1.907 | 736.7 | 2.84 | −0.0016 | 0.001 50 | 0.291 81 | −738.708 20 |
| | aug-cc-pVQZ | 1.898 | 742.9 | 2.84 | −0.0006 | 0.001 51 | 0.294 47 | −738.767 43 |
| | aug-cc-pCVTZ | 1.901 | 734.0 | 2.78 | −0.0113 | 0.001 52 | 0.293 35 | −739.292 52 |
| | aug-cc-pCVQZ | 1.891 | 747.0 | 2.82 | −0.0044 | 0.001 52 | 0.296 82 | −739.429 94 |
| RCCSD(T)-F12 | VTZ-F12 | 1.898 | 737.9 | 2.91 | −0.0069 | 0.001 54 | 0.294 36 | −738.663 67 |
| | | | | $PS^+(X^1\Sigma^+)$ | | | | |
| MRCISD | aug-cc-pVTZ | 1.845 | 819.9 | 3.20 | −0.0010 | 0.001 57 | 0.311 72 | −738.318 58 |
| | aug-cc-pVQZ | 1.834 | 833.2 | 3.16 | −0.0016 | 0.001 55 | 0.315 31 | −738.341 42 |
| | aug-cc-pV5Z | 1.828 | 839.0 | 3.15 | 0.0003 | 0.001 55 | 0.317 33 | −738.350 10 |
| RCCSD(T) | aug-cc-pVTZ | 1.842 | 825.8 | 3.10 | 0.0017 | 0.001 55 | 0.312 53 | −738.339 43 |
| | aug-cc-pVQZ | 1.831 | 839.8 | 3.05 | −0.0036 | 0.001 53 | 0.316 29 | −738.364 97 |
| | aug-cc-pV5Z | 1.825 | 845.6 | 3.07 | 0.0012 | 0.001 54 | 0.318 33 | −738.374 85 |
| | aug-cc-pV(T+d)Z | 1.835 | 831.4 | 3.07 | −0.0023 | 0.001 55 | 0.315 06 | −738.344 57 |
| | aug-cc-pV(Q+d)Z | 1.827 | 843.6 | 3.06 | −0.0032 | 0.001 54 | 0.317 70 | −738.368 05 |
| | aug-cc-pVTZ-DK | 1.835 | 832.2 | 3.06 | −0.0037 | 0.001 55 | 0.315 14 | −737.867 88 |
| | aug-cc-pVQZ-DK | 1.826 | 844.8 | 3.07 | 0.0004 | 0.001 54 | 0.318 16 | −738.364 98 |
| | aug-cc-pCVTZ | 1.835 | 831.4 | 3.04 | −0.015 39 | 0.001 57 | 0.315 02 | −738.345 84 |
| | aug-cc-pCVQZ | 1.826 | 844.2 | 2.98 | −0.007 99 | 0.001 53 | 0.318 04 | −738.369 76 |
| RCCSD(T)/ core0 | aug-cc-pVTZ | 1.837 | 836.1 | 3.04 | 0.0003 | 0.001 52 | 0.314 39 | −738.420 52 |
| | aug-cc-pVQZ | 1.828 | 844.1 | 3.11 | 0.0025 | 0.001 53 | 0.317 30 | −738.478 33 |
| | aug-cc-pCVTZ | 1.831 | 835.4 | 3.13 | 0.0043 | 0.001 55 | 0.316 33 | −739.004 56 |
| | aug-cc-pCVQZ | 1.821 | 849.4 | 3.17 | 0.0109 | 0.001 55 | 0.3199 | −739.140 59 |
| RCCSD(T)-F12 | VTZ-F12 | 1.828 | 839.6 | 3.14 | −0.0035 | 0.001 56 | 0.317 24 | −738.374 67 |
| | | | | $PS^-(X^3\Sigma^-)$ | | | | |
| MRCISD | aug-cc-pVTZ | 2.019 | 589.7 | 2.54 | 0.0028 | 0.001 54 | 0.260 21 | −738.640 26 |
| | aug-cc-pVQZ | 2.006 | 600.2 | 2.57 | 0.0002 | 0.001 55 | 0.263 49 | −738.663 49 |
| | aug-cc-pV5Z | 2.000 | 604.5 | 2.54 | 0.0011 | 0.001 54 | 0.265 17 | −738.671 76 |
| RCCSD(T) | aug-cc-pVTZ | 2.013 | 599.2 | 2.38 | −0.0035 | 0.001 49 | 0.261 65 | −738.684 40 |
| | aug-cc-pVQZ | 2.000 | 610.8 | 2.48 | 0.0066 | 0.001 50 | 0.265 25 | −738.711 77 |
| | aug-cc-pV5Z | 1.993 | 615.2 | 2.42 | 0.0024 | 0.001 49 | 0.267 03 | −738.721 83 |
| | aug-cc-pV(T+d)Z | 2.005 | 603.4 | 2.42 | 0.001 13 | 0.0015 | 0.263 91 | −738.688 08 |
| | aug-cc-pV(Q+d)Z | 1.995 | 613.3 | 2.461 | 0.0021 | 0.001 51 | 0.266 53 | −738.714 16 |
| | aug-cc-pVTZ-DK | 2.005 | 603.0 | 2.40 | 0.0008 | 0.001 50 | 0.263 85 | −738.198 59 |
| | aug-cc-pVQZ-DK | 1.993 | 614.6 | 2.46 | 0.0033 | 0.001 50 | 0.266 97 | −738.214 49 |
| | aug-cc-pCVTZ | 2.005 | 602.9 | 2.37 | −0.0052 | 0.001 50 | 0.263 85 | −738.689 55 |
| | aug-cc-pCVQZ | 1.994 | 613.9 | 2.45 | 0.0001 | 0.001 51 | 0.266 84 | −738.715 82 |
| RCCSD(T)/ core0 | aug-cc-pVTZ | 2.004 | 610.2 | 2.51 | 0.0074 | 0.001 50 | 0.264 08 | −738.763 64 |
| | aug-cc-pVQZ | 1.996 | 613.7 | 2.46 | 0.0020 | 0.001 51 | 0.266 32 | −738.824 19 |
| | aug-cc-pCVTZ | 2.001 | 605.5 | 2.37 | −0.0058 | 0.001 51 | 0.265 01 | −739.347 94 |
| | aug-cc-pCVQZ | 1.988 | 616.8 | 2.45 | 0.0011 | 0.001 51 | 0.268 38 | −739.486 32 |
| RCCSD(T)-F12 | VTZ-F12 | 1.996 | 608.3 | 2.55 | −0.0008 | 0.001 55 | 0.266 14 | −738.719 23 |

(=2.86 $cm^{-1}$). The equilibrium distance exhibits very small deviations with the data of Jenouvrier and Pascat[5] by less than 0.001 Å. This good agreement is also reflected in rotational constant ($B_{e,\ RCCSD(T)\text{-}F12/VTZ\text{-}F12}$ = 0.294 36 $cm^{-1}$ and $B_{e,\ exp.}$ = 0.2976 $cm^{-1}$).

There exists only one experimental value available for $PS^+$ ($X^1\Sigma^+$), the earlier harmonic wavenumber determined by Dressler and Miescher[1,2] ($\omega_e$ = 844.6 $cm^{-1}$). The $\omega_e$ obtained at CCSD(T)-F12/VTZ-F12 is equal to 839.6 $cm^{-1}$ differing by 5 $cm^{-1}$ from the experimental value. Both are close to the MRD-CI $\omega_e$ value (=837.9 $cm^{-1}$) by Karna *et al.*[12] The other parameters given in Table I represent predictions for this cation.

Interestingly, there are no experimental geometric parameters to compare with the RCCSD(T)-F12 structure for $PS^-$. However, Bruna and Grein[13] reported a value of 2.053 Å for the (P-S) bond distance from a MRD-CI calculation and an harmonic wavenumber, $\omega_e$ of 570 $cm^{-1}$. The ROHF/6-31G*(6d) calculations by Moussaoui *et al.*[10] lead to a (P-S) bond length of 2.0127 Å and $\omega_e$ = 667 $cm^{-1}$. The calculated RCCSD(T)-F12 values are: P-S equilibrium distance = 1.996 Å and $\omega_e$ = 608.3 $cm^{-1}$. The (P-S) distance is shorter than previous theoretical values and the present $\omega_e$ falls in between theirs. These results should be helpful in the experimental characterization of this anion in laboratory and in the interstellar medium.

Table II gives the IE and the adiabatic EA of PS. The ionization energies in this table are calculated as the difference at 0 K between the total energies of the cation and the corresponding neutral, i.e., IE = $E_0$(cation)-$E_0$(neutral), using equilibrium geometries from the same level of theory. Similarly, the EAs are calculated as the difference in total energies at 0 K of the anion and the corresponding neutral at the respective levels of theory, i.e., EA = $E_0$(neutral) $-E_0$(anion) including the zero point correction evaluated variationally.

The adiabatic ionization energies of PS in Table II, obtained at the coupled cluster level of theory, are ~7.8 eV, that is ~0.3 eV above the present MRCISD and the MRD-CI result.[13] The (R)CCSD(T)-F12 value is 7.870 eV that is 0.33 eV above the MRD-CI result. The earlier estimated ionization energy by Drowart *et al.*[6] of 9 eV is out of the range of the present computed values. This quantity should be measured again by means of photoelectron spectroscopic techniques for better accuracy. The adiabatic EA of PS is estimated to be 1.52 eV at the (R)CCSD(T)-F12 level of theory (see Table II), rather close to the value of 1.60 eV reported by Bruna and Grein[13] and to the CAS-ACPF value of 1.423 eV by Klacher.[11] Again, the MRCISD and MRD-CI EAs are off by ~0.35 eV.

For both IE and EA, the present work shows that the inclusion of the core electron correlation does not affect significantly the calculated IEs and EAs, as the (R)CCSD(T)/core 0 values in Table II are close to the (R)CCSD(T) values calculated with the same basis set, but without core electron correlation. The inclusion of the tight d functions or the scalar relativistic effects within the Douglas Kroll approximation has also a quite limited impact on the computation of these quantities. See Table II for more details.

TABLE II. Ionization energy (IE in eV) and adiabatic electron affinity (EA in eV) for PS. We included the zero point vibrational energy (ZPE) correction.

| Method | Basis set | IE | EA |
|---|---|---|---|
| MRCISD | aug-cc-pVTZ | 7.566 | 1.201 |
| | aug-cc-pVQZ | 7.567 | 1.211 |
| | aug-cc-pV5Z | 7.571 | 1.196 |
| RCCSD(T) | aug-cc-pVTZ | 7.854 | 1.547 |
| | aug-cc-pVQZ | 7.886 | 1.565 |
| | aug-cc-pV5Z | 7.888 | 1.567 |
| | aug-cc-pV(T+d)Z | 7.839 | 1.522 |
| | aug-cc-pV(Q+d)Z | 7.877 | 1.554 |
| | aug-cc-pVTZ-DK | 7.858 | 1.545 |
| | aug-cc-pVQZ-DK | 7.884 | 1.562 |
| | aug-cc-pCVTZ | 7.842 | 1.525 |
| | aug-cc-pCVQZ | 7.877 | 1.553 |
| RCCSD(T) / core0 | aug-cc-pVTZ | 7.834 | 1.516 |
| | aug-cc-pVQZ | 7.873 | 1.552 |
| | aug-cc-pCVTZ | 7.842 | 1.516 |
| | aug-cc-pCVQZ | 7.880 | 1.542 |
| RCCSD(T)-F12 | VTZ-F12 | 7.870 | 1.520 |
| Calc. | | 7.54[a] | 1.18[b] |
| Calc. | | | 1.60[c] |
| Calc. | | | 1.423[d] |
| Exp. | | ~9[e] | |

[a]MRD-CI (Ref. 12).
[b]MRD-CI (Ref. 13).
[c]Best estimate from Ref. 13.
[d]CAS-ACPF (Ref. 11).
[e]Approximate estimate by Drowart *et al.*[6]

## IV. ELECTRONIC EXCITED STATES OF PS, $PS^+$, AND $PS^-$: POTENTIALS AND SPECTROSCOPY

Table III lists the dominant electron configuration of the electronic states of PS, $PS^+$, and $PS^-$ of interest in the present study. Table S1 of the supplementary material[58] gives the composition of the wavefunctions of the electronic states of PS, $PS^+$, and $PS^-$ at equilibrium and large internuclear distances ($R_{PS}$ = 5 $a_0$) with their corresponding weights. This table shows that close to equilibrium the electronic states are dominantly described by one electronic configuration for all three molecular species except for PS($3^2\Pi$, $4^2\Pi$, $3^2\Sigma^+$) states which have a multi-reference character. Therefore, the spectroscopic parameters of these monoconfigurational states, which are computed using the derivatives of the potential close to equilibrium, can be computed by coupled clusters approaches. For large internuclear distances, the majority of the electronic wavefunctions present however a multi-reference character.

Tables IV–VI present the MRCI transition energies ($T_0$, including the zero point vibrational energy) of the bound electronic states of these molecular species. Generally, the $T_0$ values are expected to be accurate to within ~0.05 eV for the lower states and to within ~0.1 eV for the higher states according to our experience in computing such quantity and by comparing our values with the experimentally determined transition energies for other molecular diatomics.

TABLE III. Dominant electronic configurations of the electronic states of PS, $PS^-$, and $PS^+$ investigated presently.

| PS | | $PS^-$ | | $PS^+$ | |
|---|---|---|---|---|---|
| States | Electronic configuration | States | Electronic configuration | States | Electronic configuration |
| $X^2\Pi$ | $(8\sigma^2)(9\sigma^2)(3\pi^4)(4\pi^1)$ | $X^3\Sigma^-$ | $(8\sigma^2)(9\sigma^2)(3\pi^4)(4\pi^2)$ | $X^1\Sigma^+$ | $(8\sigma^2)(9\sigma^2)(3\pi^4)$ |
| $1^4\Pi$ | $(8\sigma^2)(9\sigma^2)(3\pi^3)(4\pi^2)$ | $1^1\Delta$ | $(8\sigma^2)(9\sigma^2)(3\pi^4)(4\pi^2)$ | $1^3\Sigma^+$ | $(8\sigma^2)(9\sigma^2)(3\pi^3)(4\pi^1)$ |
| $2^2\Pi$ | $(8\sigma^2)(9\sigma^2)(3\pi^3)(4\pi^2)$ | $1^1\sum^+$ | $(8\sigma^2)(9\sigma^1)(3\pi^4)(4\pi^2)$ | $1^3\Delta$ | $(8\sigma^2)(9\sigma^2)(3\pi^3)(4\pi^1)$ |
| $1^4\Sigma^-$ | $(8\sigma^2)(9\sigma^1)(3\pi^4)(4\pi^2)$ | $1^3\Pi$ | $(8\sigma^2)(9\sigma^2)(10\sigma^1)(3\pi^4)(4\pi^1)$ | $1^3\Sigma^-$ | $(8\sigma^2)(9\sigma^2)(3\pi^3)(4\pi^1)$ |
| $1^2\Phi$ | $(8\sigma^2)(9\sigma^2)(3\pi^3)(4\pi^2)$ | $1^1\Pi$ | $(8\sigma^2)(9\sigma^2)(10\sigma^1)(3\pi^4)(4\pi^1)$ | $1^1\Sigma^-$ | $(8\sigma^2)(9\sigma^2)(3\pi^3)(4\pi^1)$ |
| $3^2\Pi$ | $(8\sigma^2)(9\sigma^2)(3\pi^3)(4\pi^2)$ | $1^1\ \Sigma^-$ | $(8\sigma^2)(9\sigma^2)(3\pi^3)(4\pi^3)$ | $1^3\Pi$ | $(8\sigma^2)(9\sigma^1)(3\pi^4)(4\pi^1)$ |
| $1^2\Sigma^+$ | $(8\sigma^2)(9\sigma^2)(10\sigma^1)(3\pi^4)$ | $1^3\Delta$ | $(8\sigma^2)(9\sigma^2)(3\pi^3)(4\pi^3)$ | $1^1\Delta$ | $(8\sigma^2)(9\sigma^2)(3\pi^3)(4\pi^1)$ |
| $1^2\Delta$ | $(8\sigma^2)(9\sigma^1)(3\pi^4)(4\pi^2)$ | $1^3\Sigma^+$ | $(8\sigma^2)(9\sigma^2)(3\pi^3)(4\pi^3)$ | $1^1\Pi$ | $(8\sigma^2)(9\sigma^1)(3\pi^4)(4\pi^1)$ |
| $1^2\Sigma^-$ | $(8\sigma^2)(9\sigma^1)(3\pi^4)(4\pi^2)$ | $1^5\Pi$ | $(8\sigma^2)(9\sigma^2)(10\sigma^1)(3\pi^3)(4\pi^2)$ | $2^1\Sigma^+$ | $(8\sigma^2)(9\sigma^2)(3\pi^2)(4\pi^2)$ |
| $2^2\Sigma^+$ | $(8\sigma^2)(9\sigma^1)(3\pi^4)(4\pi^2)$ | $1^5\Sigma^-$ | $(8\sigma^2)(9\sigma^1)(10\sigma^1)(3\pi^4)(4\pi^2)$ | $1^5\Pi$ | $(8\sigma^2)(9\sigma^1)(3\pi^3)(4\pi^2)$ |
| $4^2\Pi$ | $(8\sigma^2)(9\sigma^2)(3\pi^3)(4\pi^2)$ | | | | |
| $3^2\Sigma^+$ | $(8\sigma^2)(9\sigma^2)(10\sigma^1)(3\pi^3)(4\pi^1)$ | | | | |
| $1^4\Sigma^+$ | $(8\sigma^2)(9\sigma^2)(10\sigma^1)(3\pi^3)(4\pi^1)$ | | | | |
| $1^4\Delta$ | $(8\sigma^2)(9\sigma^1)(3\pi^3)(4\pi^3)$ | | | | |
| $1^6\Sigma^+$ | $(8\sigma^2)(9\sigma^2)(10\sigma^1)(3\pi^2)(4\pi^2)$ | | | | |
| $1^6\Pi$ | $(8\sigma^2)(9\sigma^1)(10\sigma^1)(3\pi^3)(4\pi^2)$ | | | | |

TABLE IV. CASSCF/MRCI/aug-ccpV5Z adiabatic transition energy ($T_0$ in eV), including zero point vibrational energies determined variationally, the equilibrium distance ($R_e$ in Å) and the spectroscopic parameters ($\omega_e$, $\omega_e x_e$, $\omega_e y_e$, $G_0$, $\alpha_e$, $B_e$, in $cm^{-1}$) and the spin-orbit constant at equilibrium ($A_{SO}$) of PS.

| State | $T_0$ | $R_e$ | $\omega_e$ | $\omega_e x_e$ | $\omega_e y_e$ | $G_0$ | $\alpha_e$ | $B_e$ | $A_{SO}$ |
|---|---|---|---|---|---|---|---|---|---|
| $X^2\Pi$ | 0.0 | 1.879 | 732.0 | 2.98 | 0.0052 | 365.3 | 0.0015 | 0.2936 | 291.4 |
| | | 1.944[a] | 735.6[a] | 3.6[a] | | | | 0.2836[a] | |
| | | 1.899[b] | 739.5[b] | 2.86[b] | | | | 0.2976[b] | |
| | | | | | | | | | 320.8[c] |
| | | | | | | | | | 315.4[d] |
| $1^4\Pi$ | 2.33 | 2.14 | 496.3 | 5.54 | 0.6106 | 246.5 | 0.0013 | 0.2317 | − 109.0 |
| | 1.94[a] | 2.185[a] | 464.6[a] | 5.6[a] | | | | 0.2244[a] | |
| $2^2\Pi$ | 2.83 | 2.107 | 507.8 | 1.84 | 0.0063 | 253.5 | 0.0013 | 0.2335 | 62.0 |
| | 2.6[a] | 2.183[a] | 483.0[a] | 1.41[a] | | | | 0.2248[a] | |
| | 2.79[b] | 2.133[b] | 509.9[b] | 1.80[b] | | | | 0.2355[b] | |
| $1^4\sum^-$ | 3.37 | 2.00 | 544.4 | 2.62 | 0.1012 | 271.6 | 0.0020 | 0.2631 | |
| | 3.03[a] | 2.071[a] | 546.4[a] | 4.6[a] | | | | 0.2499[a] | |
| $1^2\Phi$ | 3.38 | 2.11 | 492.2 | 2.21 | 0.0001 | 245.6 | 0.0014 | 0.2317 | − 110.9 |
| | 3.24[a] | 2.218[a] | 473.4[a] | 8.0[a] | | | | 0.2176[a] | |
| $3^2\Pi$ | 4.11 | 2.12 | 486.4 | 2.19 | 0.0028 | 242.7 | 0.001 45 | 0.2304 | − 209.6 |
| | 3.92[a] | 2.195[a] | 525.4[a] | 5.0[a] | | | | 0.2224[a] | |
| $1^2\sum^+$ | 4.17 | 2.09 | 344.4 | 4.24 | 0.0736 | 170.5 | 0.0017 | 0.2372 | |
| | 4.01[a] | 2.345[a] | 277.3[a] | 2.0[a] | | | | 0.1946[a] | |
| $1^2\Delta$ | 4.39 | 2.00 | 533.4 | 6.55 | 0.5343 | 265.0 | 0.0021 | 0.2573 | − 0.28 |
| | 4.30[a] | 2.087[a] | 483.8[a] | 2.4[a] | | | | 0.2459[a] | |
| | 4.30[e] | 2.013[e] | 534.8[f] | 3.31[e] | | | | 0.2644[e] | |
| $1^2\sum^-$ | 4.53 | 2.00 | 484.1 | 1.45 | 0.1705 | 241.9 | 0.0019 | 0.2445 | |
| | 4.40[a] | 2.164[a] | 472.1[a] | 4.4[a] | | | | 0.2307[a] | |
| $2^2\sum^+$ | 4.94 | 2.02 | 522.4 | 6.02 | 0.243 66 | 259.2 | 0.002 27 | 0.254 19 | |
| $4^2\Pi$ | 5.13 | 2.20 | 400.4 | 1.94 | 0.0393 | 199.7 | 0.0015 | 0.2140 | 184.0 |
| | 5.17[a] | 2.256[a] | 410.1[a] | 4.4[a] | | | | 0.2105[a] | |
| $3^2\sum^+$ | 5.74 | 2.48 | 652.9 | 34.02 | 0.5724 | 311.0 | 0.0021 | 0.1684 | |
| | 5.16[a] | 2.009[a] | 767.5[a] | 0.5[a] | | | | 0.2653[a] | |

[a]MRD-CI calculations.[8]
[b]UV emission spectroscopy. Exp. (Ref. 5).
[c]UV emission spectroscopy. Exp. (Ref. 4).
[d]CAS-ACPF calculations.[11]
[e]UV emission spectroscopy. Exp. (Refs. 1 and 2).

TABLE V. CASSCF/MRCI/aug-ccpV5Z adiabatic transition energy ($T_0$ in eV), including zero point vibrational energies determined variationally, the equilibrium distance ($R_e$ in Å) and the spectroscopic parameters ($\omega_e$, $\omega_e x_e$, $\omega_e y_e$, $G_0$, $\alpha_e$, $B_e$, in $cm^{-1}$) and the spin-orbit constant at equilibrium ($A_{SO}$) of $PS^+$.

| state | $T_0$ | $R_e$ | $\omega_e$ | $\omega_e x_e$ | $\omega_e y_e$ | $G_0$ | $B_e$ | $\alpha_e$ | $A_{SO}$ |
|---|---|---|---|---|---|---|---|---|---|
| $X^1\Sigma^+$ | 0.0 | 1.829 | 838.7 | 3.13 | 0.001 05 | 418.5 | 0.317 20 | 0.001 55 | |
| | | 1.872 | 837.9[a] | | | | 0.3055[a] | | |
| | | | 844.6[b] | | | | | | |
| $1^3\Sigma^+$ | 2.758 | 2.031 | 575.6 | 3.76 | 0.709 20 | 289.8 | 0.257 05 | 0.001 57 | |
| | 2.48[a] | 2.083[a] | 649.1[a] | | | | 0.2469[a] | | |
| $1^3\Delta$ | 3.433 | 2.027 | 587.3 | 5.34 | 0.897 80 | 296.2 | 0.258 28 | 0.001 57 | − 2.5 |
| | 3.27[a] | 2.074[a] | 621.4[a] | | | | 0.2492[a] | | |
| $1^3\Sigma^-$ | 3.911 | 2.032 | 579.0 | 3.67 | 0.643 30 | 291.5 | 0.256 76 | 0.001 45 | |
| | 3.73[a] | 2.080[a] | 611.2[a] | | | | 0.2476[a] | | |
| $1^1\Sigma^-$ | 3.952 | 2.034 | 587.1 | 2.90 | 0.011 40 | 292.8 | 0.256 46 | 0.001 53 | |
| | 3.83[a] | 2.092[a] | 566.3[a] | | | | 0.2447[a] | | |
| $1^3\Pi$ | 4.114 | 1.911 | 663.1 | 3.72 | 0.043 60 | 330.6 | 0.290 36 | 0.001 99 | 163.5 |
| | 3.92[a] | 1.966[a] | 613.8[a] | | | | 0.2769[a] | | |
| $1^1\Delta$ | 4.143 | 2.034 | 575.7 | 3.20 | 0.014 21 | 286.9 | 0.256 34 | 0.001 61 | |
| | 3.99[a] | 2.104[a] | 533.7[a] | | | | 0.2420[a] | | |
| $1^1\Pi$ | 5.093 | 1.951 | 595.8 | 4.56 | 0.043 64 | 296.7 | 0.278 77 | 0.002 25 | |
| | 5.03[a] | 1.977[a] | 523.0[a] | | | | 0.2687[a] | | |
| | 5.03[b] | | 607.5[b] | | | | | | |
| $2^1\Sigma^+$ | 5.55 | 2.346 | 366.5 | 0.99 | 0.022 19 | 183.1 | 0.192 73 | 0.000 91 | |
| | 5.21[a] | 2.322[a] | 591.5[a] | | | | 0.1933[a] | | |
| $1^5\Pi$ | 5.788 | 2.25 | 330.4 | 2.52 | 0.002 74 | 164.7 | 0.209 11 | 0.002 25 | − 91.2 |
| | 5.15[a] | 2.345[a] | 284.0[a] | | | | 0.1955[a] | | |

[a]MRD-CI calculations (Ref. 12).
[b]UV emission spectroscopy. Exp. (Refs. 1 and 2).

The evolutions along the internuclear distance of the potential energy curves and of the spin-orbit couplings integrals of PS, PS+, and PS− are depicted in Figures 1, 3, and 5, respectively; and a set of spectroscopic constants for each are given in Tables IV–VI. Figures 2 and 4 show the evolution along the internuclear distance of the diagonal and some off-diagonal spin-orbit integrals involving the lowest electronic states of PS, $PS^+$. Figure 6 displays the diagonal and the off-diagonal spin-orbit integrals of $PS^-$ which present non-zero spin-orbit integral. In Figures 2, 4, and 6, the following notation is used: A-B denotes the $\langle A|\mathbf{H^{SO}}|B\rangle$ integral. For instance, the $X^2\Pi$-$X^2\Pi$ term of PS corresponds to the $\langle X^2\Pi|\mathbf{H^{SO}}|X^2\Pi\rangle$ integral. These integrals evolve smoothly (either constant or increase monotonically) along the P-S internuclear distance. The spin-orbit constants ($A_{SO}$) at equilibrium can be deduced from the corresponding diagonal spin-orbit integrals evaluated at equilibrium by using the formula $A_{SO,e}\ (^{2\Sigma+1}\Lambda) = \langle ^{2\Sigma+1}\Lambda|\mathbf{H^{SO}}|^{2\Sigma+1}\Lambda\rangle/\Lambda\Sigma$ (for $\Lambda \neq 0$ and $\Sigma \neq 0$).[56]

### A. The PS radical

The full set of the CASSCF/MRCI/aug-ccpV5Z potential energy curves of PS vs. the internuclear distance are depicted in Figure 1. These potentials are given in energy with respect to the GS minimum. We considered electronic states that converge adiabatically to the $P(^4S_u)$ + $S(^3P_g)$, $P(^4S_u)$ + $S(^1D_g)$, $P(^2D_u)$ + $S(^3P_g)$ asymptotes. Generally, the pattern of the electronic states located in the domain of interest is in good accord with those previously computed. Exception

TABLE VI. CASSCF/MRCI/aug-ccpV5Z adiabatic transition energy ($T_0$ in eV), including zero point vibrational energies determined variationally, the equilibrium distance ($R_e$ in Å) and the spectroscopic parameters ($\omega_e$, $\omega_e x_e$, $\omega_e y_e$, $G_0$, $\alpha_e$, $B_e$, in $cm^{-1}$) of $PS^-$.

| State | $T_0$ | $R_e$ | $\omega_e$ | $\omega_e x_e$ | $\omega_e y_e$ | $G_0$ | $B_e$ | $\alpha_e$ |
|---|---|---|---|---|---|---|---|---|
| $X^3\Sigma^-$ | 0.0 | 2.000 | 604.5 | 2.54 | 0.001 20 | 301.6 | 0.265 17 | 0.001 54 |
| | 0.0[a] | 0.254[a] | 570[a] | 3.3[a] | | | 2.053[a] | 0.0013[a] |
| $1^1\Delta$ | 0.57 | 1.997 | 606.6 | 2.57 | 0.001 49 | 302.7 | 0.266 08 | 0.001 55 |
| | 0.50[a] | 2.042[a] | 610[a] | 3.3[a] | | | 0.256[a] | 0.0014[a] |
| $1^1\Sigma^+$ | 0.96 | 1.999 | 596.5 | 2.77 | 0.000 37 | 297.5 | 0.265 37 | 0.001 62 |
| | 0.91[a] | 2.042[a] | 600[a] | 3.0[a] | | | 0.256[a] | 0.0016[a] |
| $^1\Sigma^-$ | 2.78 | 2.315 | 388.4 | 1.59 | 0.044 07 | 193.7 | 0.197 94 | 0.000 80 |
| $^3\Delta$ | 2.87 | 2.824 | 413.5 | 5.63 | 0.217 08 | 204.7 | 0.201 02 | 0.001 68 |
| $^3\Sigma^+$ | 2.94 | 2.316 | 382.9 | 0.32 | 0.469 75 | 191.5 | 0.000 97 | 0.000 97 |

[a]MRD-CI calculations (Ref. 13).

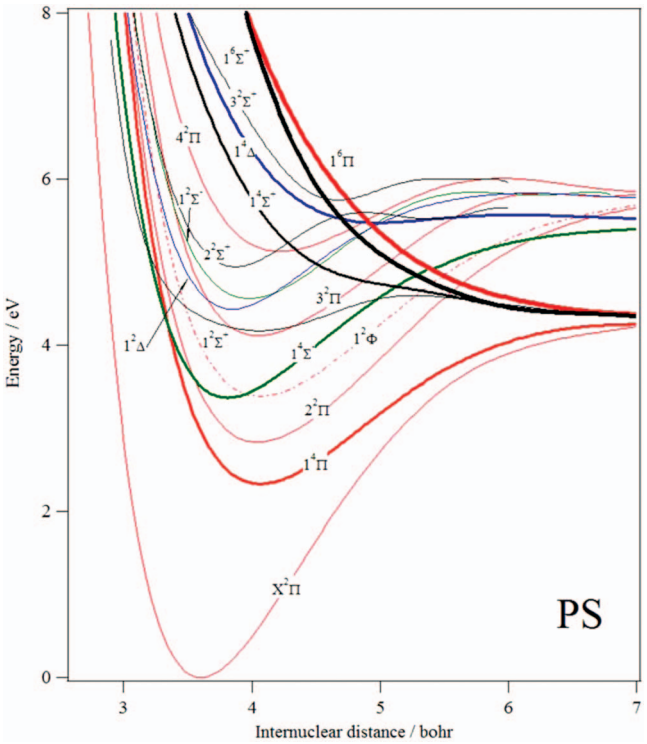


FIG. 1. CASSCF/MRCI/aug cc-pV5Z potential energy curves of the doublet (thin lines), quartet (thick lines), and the sextet (thickest lines) electronic states of PS correlating to the two lowest dissociation limits. These PECs are given in energy with respect to the energy of PS($X^2\Pi$) at equilibrium.

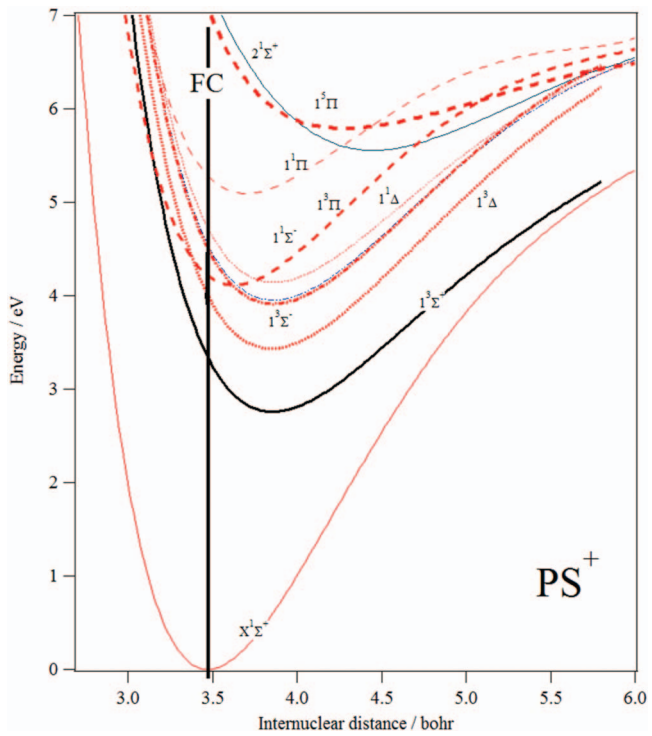


FIG. 3. CASSCF/MRCI/aug cc-pV5Z potential energy curves of the singlet (thin lines), triplet (thick lines), and quintet (thickest lines) electronic states of $PS^+$. These PECs are given in energy with respect to the energy of $PS^+(X^1\Sigma^+)$ at equilibrium. The solid thick vertical line represents the middle of the Franck-Condon region accessed from the ground state of $PS^+$.

exists for the $4^2\Pi$ and $3^2\Sigma^+$ electronic states which are high in energy. For PS($4^2\Pi$), there is *one* unique potential well instead of two potential wells as seen in Ref. 8. For PS($3^2\Sigma^+$), we compute a potential well for internuclear distance $> 4$ $a_0$ ($1\ a_0 = 1$ bohr $= 0.5292$ Å) whereas Karna *et al.*[8] computed a potential well for $R_{PS} < 4$ $a_0$ in addition to the potential minima for $R_{PS} > 4$ $a_0$. Our analysis shows that these two electronic states present a strong valence-Rydberg mixing character, which is accounted for in the present computations and not in those of Karna *et al.*[8] Strictly speaking, our computations are much larger than those previously published so they are expected to provide more reliable data. We showed recently that the correct description of the shape of electronic states

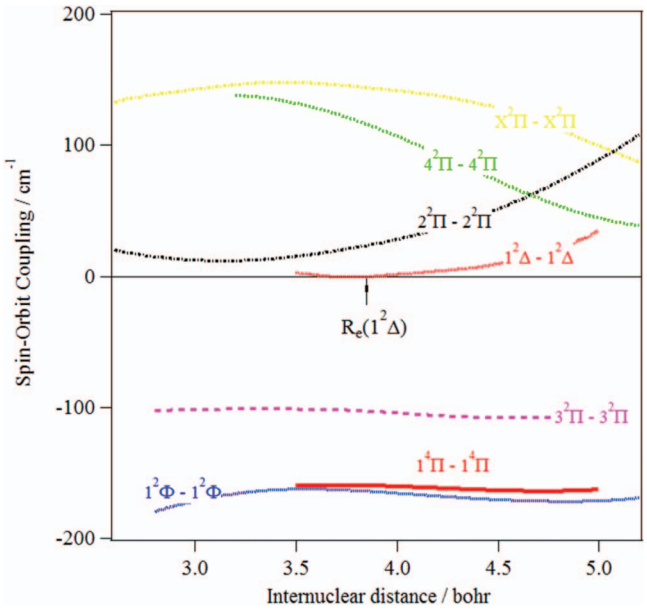


FIG. 2. Evolution of the diagonal spin-orbit integrals of the electronic states of PS. See text for more details.

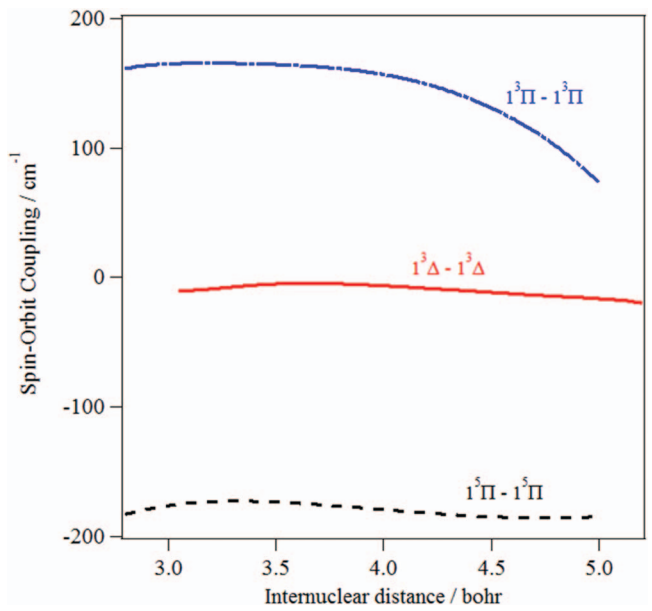


FIG. 4. Evolution of the diagonal spin-orbit integrals of the electronic states of $PS^+$. See text for more details.

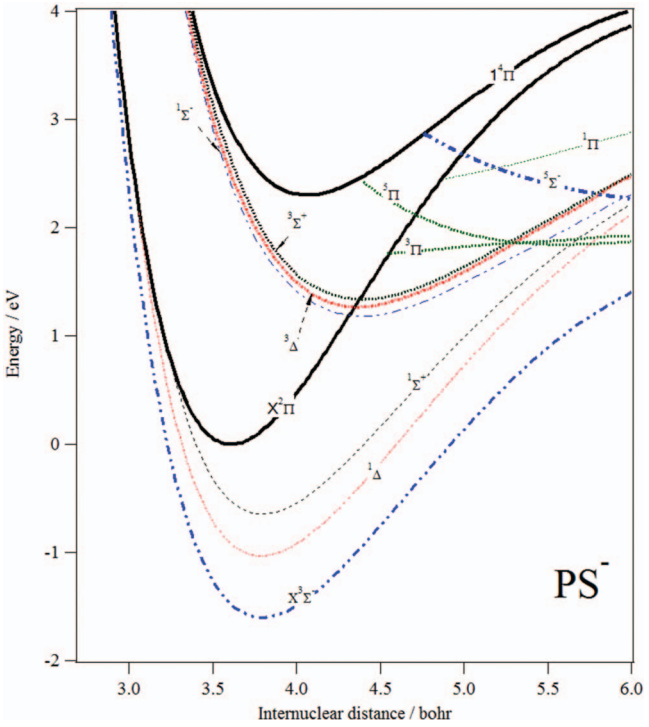


FIG. 5. CASSCF/MRCI/aug cc-pV5Z potential energy curves of the stable and metastable electronic states of $PS^-$. We are also giving those of the corresponding neutral parent states (thick black solid lines, see text for more details). These PECs are given in energy with respect to the energy of $PS(X^2\Pi)$ at equilibrium. The initially *ab initio* computed anionic PECs were shifted by −0.62 eV in order to match the experimental EA of $PS^-$ ($X^3\Sigma^-$) (see text).

located well above GS is critical for the accurate prediction of unimolecular decomposition processes and of cold atom and molecule productions.[57]

For the ground state of PS, the present work reports a value of $A_{SO}$ ($X^2\Pi$) = 291.4 $cm^{-1}$, which is off by 9% from the experimental value of 320.8 $cm^{-1}$ (Table IV).[4] This deviation corresponds to the standard error that one may expect for such calculations. The computed $A_{SO}$ values for the $^2\Pi$, $^2\Delta$, $^2\Phi$, and $^4\Pi$ upper electronic states are probably 10% lower than the exact $A_{SO}$. Hence, it is recommend to add 10% to the reported values to get a better estimate of these quantities. Figure S1 of the supplementary material[58] gives the evolution of some non-vanishing off-diagonal spin-orbit integrals of PS vs. the $R_{PS}$ distance that may be helpful for discussing the metastability and the spin-orbit predissociation processes at high energies.

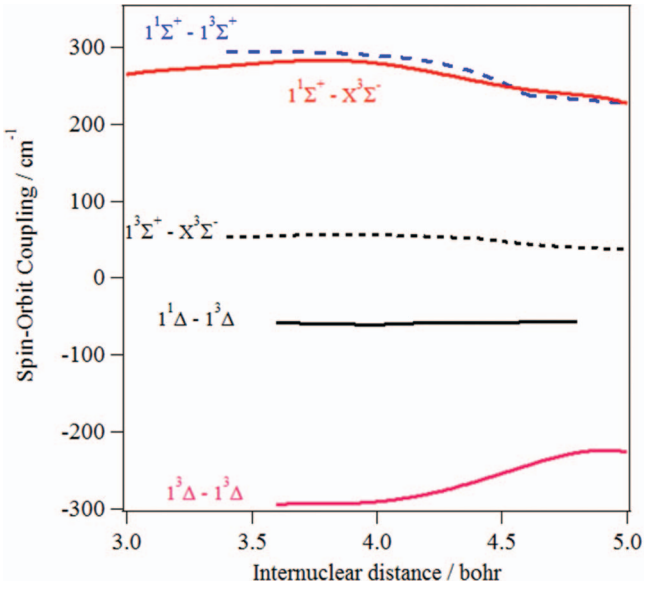


FIG. 6. Evolution of the diagonal and non-vanishing off-diagonal spin-orbit integrals of the electronic states of $PS^-$. See text for more details.

Table IV presents the spectroscopic parameters of the bound electronic states of PS, which are deduced from a state-averaging CASSCF/MRCI procedure and their comparison to the theoretical results by Karna *et al.*[8] and to those deduced experimentally. The $R_e$ of 1.879 Å for PS ($X^2\Pi$) is closer to the $R_e$ derived experimentally by Jenouvrier and Pascat[5] being 1.899 Å than that computed by Karna *et al.*[8] (=1.944 Å). The harmonic wavenumber is computed 732.0 $cm^{-1}$, which is in close accord with the 735.6 and 739.5 $cm^{-1}$ of Refs. 5 and 8. Similarly the anharmonic term ($\omega_e x_e$) agrees with theirs. For the $2^2\Pi$ state (the B state), our transition energy (of 2.83 eV), $R_e$ (of 2.107 Å), $\omega_e$ (of 507.8 $cm^{-1}$), and $\omega_e x_e$ (of 1.984 $cm^{-1}$) are in excellent accord with those determined experimentally by Jenouvrier and Pascat[5] (see Table IV). However, the corresponding values from Karna *et al.* show larger deviations, which attest to the good accuracy of the present calculations.

Interestingly, the transition energy computed for the $1^2\Delta$ state ($T_0$ = 4.39 eV) coincides, after consideration of the error bars of the present computations, with that measured by Dressler and Miescher[1,2] and by Narasimham and Balasubramanian[3,4] (i.e., $T_0$ = 4.30 eV) for the UV band ($X \leftarrow C$ transition). This band was attributed there to the emission from the $2^2\Sigma^+$ rather than from the $1^2\Delta$ state. The equilibrium distance and the harmonic wavenumber computed for $1^2\Delta$ ($R_e$ = 2.00 Å, $\omega_e$ = 533.4 $cm^{-1}$) are close to those derived from the analysis of this band (i.e., $R_e$ = 2.013 Å, $\omega_e$ = 534.8 $cm^{-1}$). This suggests a new assignment for this transition as an emission transition from the $1^2\Delta$ state to populate the electronic ground state. Several other arguments can be given for this reassignment. Indeed, the $2^2\Sigma^+$ is located at 4.94 eV above ground state: the corresponding transition energy is off by 0.6 eV which is out of the error bars of these computations. In addition, Narasimham and Balasubramanian[4] described their spectrum to consist of "strong lines readily identified to the Q branch lines." Again, strong line signal for the Q branch is in favor for a $^2\Delta$ emitting state rather than a $^2\Sigma^+$ as is well established in Ref. 59. Moreover, the basic argument given by these experimentalists for this assignment to a $^2\Sigma^+$ is the absence of splitting, due to spin-orbit, in the experimental spectra. The spin-orbit coupling terms depicted in Figure 2 show that the $\langle 1^2\Delta|\mathbf{H^{SO}}|1^2\Delta\rangle$ spin-orbit coupling goes accidentally close to zero near the equilibrium distance of this electronic state (the arrow in this figure). Therefore, the "significant spin-splitting of the $^2\Sigma^+$ with $\gamma$-value of 0.017 $cm^{-1}$" emphasised by Narasimham and Balasubramanian[4] should be reconsidered in terms of spin-orbit splitting of the $1^2\Delta$ state. Finally and for the isovalent

$NO^+$ and $NS^+$ cations,[60] the corresponding transitions are assigned to a $^2\Delta$ emitting state rather than to a $^2\Sigma^+$.

### B. The $PS^+$ cation

Figure 3 displays the CASSCF/MRCI/aug cc-pV5Z potential energy curves of the $PS^+$ electronic states lying in the 0–7 eV energy domain. These curves are given with respect to the $PS^+$ $X^1\Sigma^+$ minimum energy. We compute electronic states of singlet, triplet, and quintet spin-multiplicities. These electronic states correlate mainly to the $P^+(^3P_g) + S(^3P_g)$ and $S^+(^4S_u) + P(^4S_u)$ close laying asymptotes. Table III gives their dominant electron configurations, which are quoted for the equilibrium P-S internuclear distance of $PS^+(X^1\Sigma^+)$. This table shows that the electronic states of interest are mainly formed by removing an electron from the valence $4\pi$ or $3\pi$ or $9\sigma$ molecular orbitals. These electronic states were previously investigated by Karna *et al.*;[12] the shape of the potentials are close to theirs with the exception of the $2^1\Sigma^+$. Indeed, we compute for this electronic state a shallow potential well rather than a deep potential well as given in Ref. 12. Similar to the neutral PS, this highly localized electronic state presents a Valence-Rydberg mixing character that is fully considered in the present work.

Table V gives the transition energies and the spectroscopic constants of the bound $PS^+$ states. Similar to the neutral, there is good agreement between our computed values for the ground state and those derived by Karna *et al.*[12] and those measured by Dressler and Miescher.[1,2] For the upper electronic states, there are slight differences present in $T_0$, $R_e$, $\omega_e$, and $B_e$ with those previously calculated by Karna *et al.*[12] At equilibrium, the $A_{so,e}(1^3\Delta)$, $A_{so,e}(1^3\Pi)$, and $A_{so,e}(1^5\Pi)$ spin-orbit constants of $PS^+$ are calculated $-2.5$, 163.5 $cm^{-1}$, and $-91.2$ $cm^{-1}$, respectively. For $NS^+$,[55] the $A_{so,e}(1^3\Pi)$, $A_{SO,e}(1^3\Delta)$, and $A_{SO,e}(1^5\Pi)$ spin-orbit constants at equilibrium are calculated 139.4 $cm^{-1}$, –14.0 $cm^{-1}$, and –84.8 $cm^{-1}$. For the lowest $^3\Pi_u$ $N_2$ state, a spin-orbit constant of 42.24 $cm^{-1}$ is measured[61,62] and for $N_2(C''^5\Pi_u)$, Field *et al.*[63] were measuring a $A_{SO,e}$ constant of $-16.4$ $cm^{-1}$. Therefore, the $PS^+$ spin-orbit constants are larger than those of the $NS^+$ and $N_2$ isovalent systems because of the larger spin-orbit effect in atomic sulfur and phosphorus,[56] except for the $PS^+(1^3\Delta)$ which has a close to zero value at equilibrium (Figure 4).

Experimentally, Dressler attributed the UV band relative to the $PS^+$ ion to the $X^1\Sigma^+ \leftarrow 2^1\Sigma^+$ emission transition. Figure 3 shows that the $2^1\Sigma^+$ electronic state is located outside the Franck-Condon region accessed from $PS^+(X^1\Sigma^+)$. Moreover, it is computed to lay 5.55 eV above the ionic ground state whereas the experimental transition energy is 5.03 eV. In addition, it presents a quite different harmonic wavenumber (i.e., $\omega_e = 366.5$ $cm^{-1}$) from that deduced experimentally ($\omega_e = 607.5$ $cm^{-1}$). In contrast, the $1^1\Pi$ is located in the Franck-Condon region and the $T_0$ energy for this state is 5.093 eV and $\omega_e = 595.8$ $cm^{-1}$. This close agreement with the experimental quantities suggests that the $^1\Pi$ state is a better candidate as the emitting state in this UV band. Based in these considerations, the observed experimental UV band of $PS^+$ is reassigned to the $X^1\Sigma^+ \leftarrow 1^1\Pi$ transition.

### C. The $PS^-$ anion

Figure 5 presents the MRCI potential energy curves of the electronic states of $PS^-$. This figure displays also the MRCI potential energy curves of the neutral PS ($X^2\Pi$ and $a^4\Pi$) states. The anionic states correlate to the bound dissociation limits $[S^-(^2P_u) + P(^4S_u)]$ and $P^-(^3P_g) + S(^3P_g)$. Here only the bound parts of the anionic potentials are presented, since our approach is not valid to describe accurately the negative ion resonances above the auto-detachment thresholds.[53] Initially, the potential energy curves for $PS^-$ were shifted to lower energies (by about 0.62 eV) in order to match the best estimate for the electron affinity of $PS(X^2\Pi)$.[13] Figure 5 shows that the $X^3\Sigma^-$, $^1\Delta$, $^1\Sigma^+$, $^1\Sigma^-$, $^3\Delta$, and $^3\Sigma^+$ states present deep potential wells. Their dominant electron configurations are given in Table III. By adding an electron to the $4\pi$ orbital of PS, the resulting $\pi^2$ configuration gives rise to the $PS^-(X^3\Sigma^-$, $^1\Delta$, and $^1\Sigma^+)$ electronic states. The low vibrational levels of $PS^-$ ($X^3\Sigma^-$, $^1\Delta$, and $^1\Sigma^+$) are well below their auto-detachment threshold, i.e., the energy of $PS(X^2\Pi)$ $v' = 0$. This agrees with the findings of Bruna and Grein.[13] The PS ($X^2\Pi$) state is also the parent state for $PS^-$ ($^1\Pi$ and $^3\Pi$) electronic states formed by binding an extra electron to the $10\sigma$ vacant orbital (cf. Table III). These anionic states are above the auto-detachment threshold so their lifetimes are reduced and only their long range parts are predicted to be bound. For the $^1\Sigma^-$, the $^3\Delta$, and the $^3\Sigma^+$ states, their parent neutral state is $PS(a^4\Pi)$ by binding an electron to the $4\pi$ orbital. The three anionic states are definitely below this parent neutral state. For the $^1\Sigma^-$, however, the angular momentum of the fine structure component (i.e., $J = 0$) has its counterpart in the low-lying $^1\Sigma^+$ state. Similarly, the $J = 1$ and 2 components of the $^3\Delta$ and the $^3\Sigma^+$ states may couple with their counterparts in the $X^3\Sigma^-$ and $^1\Delta$ states. Hence, the $^1\Sigma^-$, $^3\Sigma^+$ and the $^3\Delta$ ($J = 1$ and 2) will probably auto-detach rapidly to the final electronic ground state of PS. Nevertheless, the $^3\Delta$ $J = 3$ fine structure component has no lower-lying counterpart and it lies below its parent state. In addition, this electronic state exhibits relatively small spin-orbit couplings with the other electronic states of $PS^-$ (Figure 6). Long-lived $PS^-$ ions may be detected in the $^3\Delta$ state.

Table VI lists the spectroscopic constants of the $PS^-$ electronic states. The calculated $\omega_e$ value for $X^3\Sigma^-$ of 604.5 $cm^{-1}$ is larger by 34 $cm^{-1}$ than that of Bruna and Grein.[13] For the two lowest excited states, better agreement is observed with the values of Bruna and Grein.[13] New data in Table VI represent predictions that should aid in the experimental characterization of $PS^-$ ion.

The spin-orbit coupling evolutions are depicted in Figure 6. These data allow evaluating the spin-orbit constant of the $PS^-(^3\Delta)$ state at equilibrium ($A_{eSO}$ $(^3\Delta)$) and the spin-spin splitting for the $PS^-(X^3\Sigma^-)$. For $A_{eSO}$ $(^3\Delta)$, it is half the $\langle ^3\Delta|\mathbf{H^{SO}}|^3\Delta\rangle$ integral. It is computed to be $\sim -134$ $cm^{-1}$. For the spin-spin splitting of the ground anionic state, the first excited state $^1\Delta$ which is located at 0.57 eV above the X state should be ruled out since the $\langle ^1\Delta|\mathbf{H^{SO}}|^3\Sigma^-\rangle$ integral gives no contribution for $\Delta\Lambda = \pm 2$. However, the following excited state, $^1\Sigma^+$ state, which results from the $\pi^2$ electron configuration as the X and A states, contributes. Using the formula in

Ref. 56, a spin-spin splitting of 10.4 $cm^{-1}$ for $PS^-$ ($X^3\Sigma^-$) is determined. This is quite a large value and should be observable in highly resolved spectra. The good agreement found for the neutral suggests that the experimentally unknown values for $PS^-$ electronic states should be of similar accuracy. This should help in the assignment of the highly resolved IR or microwave spectra of $PS^-$ in the laboratory and hence its identification in the ISM.

## V. CONCLUSION

Extensive *ab initio* calculations have been performed to provide accurate estimates for the equilibrium distances, spectroscopic parameters, and electronic excited states of PS and ions, and for the ionization energies and electron affinities of PS. At the best level of accuracy employed in this study, the adiabatic IE is predicted to be 7.87 eV for PS, while the adiabatic electron affinity is predicted to be 1.52 eV for PS. Our results are in reasonable agreement with previous theoretical investigations for the lowest electronic states. However, the shapes of the potentials of the high lying electronic states are different. These electronic states are believed to be better described here because there is accounting of possible Valence-Rydberg character contributions to these states. This has allowed for a reassignment of the earlier ultraviolet bands measured by Dressler and Miescher[1,2] for PS and $PS^+$. Long lived metastable $PS^-$ is predicted to exist, and these findings should motivate new experimental studies to characterize this potentially important astrophysical species. The spectroscopic relevant information including rotational constants, vibrational terms, spin-orbit, and spin-spin constants provided presently should aid in the detection of these molecules in the near future.

For PS and $PS^+$, Figures 1 and 3 show high density of electronic states located for energies greater than 2.5 eV. This high density should favor their mutual interactions and the mixings of their wavefunctions by vibronic, spin-orbit, Coriolis, and rotational couplings. Finally, Figure 5 reveals the high density of electronic states of $PS^-$ for $R_{PS} > 4.5\ a_0$, favoring their mutual interactions such as spin-orbit and vibronic couplings which should play a crucial role during the collisions between $S^-$ and P and between $P^-$ and S species.

## ACKNOWLEDGMENTS

M.H. thanks a financial support from the PCMI program (INSU, CNRS, FRANCE).

[1]K. Dressler and E. Miescher, Proc. Phys. Soc. A **68**, 542 (1955).
[2]K. Dressler, Helv. Phys. Acta **28**, 563 (1955).
[3]N. A. Narasimham and T. K. Balasubramanian, J. Mol. Spectrosc. **29**, 294 (1969).
[4]N. A. Narasimham and T. K. Balasubramanian, J. Mol. Spectrosc. **37**, 371 (1971).
[5]A. Jenouvrier and B. Pascat, Can. J. Phys. **56**, 1088 (1978).
[6]J. Drowart, C. E. Myers, R. Szwarc, A. Vander Auwera-Mahieu, and O. M. Uy, High Temp. Sci. **5**, 482 (1973).
[7]H. Klein, E. Klisch, and G. Winnewisser, Z. Naturforsch. **54a**, 137 (1999).
[8]S. P. Karna, P. J. Bruna, and F. Grein, J. Phys. B **21**, 1303 (1988).
[9]S. P. Karna and F. Grein, Mol. Phys. **77**, 135 (1992).
[10]Y. Moussaoui, O. Ouamerali, and G. R. De Maré, J. Mol. Struct.: THEOCHEM **425**, 237 (1998).
[11]J. Klacher, Phys. Chem. Chem. Phys. **4**, 3311 (2002).
[12]S. P. Karna, P. J. Bruna, and F. Grein, Chem. Phys. **123**, 85 (1988).
[13]P. J. Bruna and F. Grein, J. Phys. B **20**, 5967 (1987).
[14]L. M. Ziurys, Proc. Natl. Acad. Sci. U.S.A. **103**, 12274 (2006).
[15]D. Smith, Philos. Trans. R. Soc. London **324**, 257 (1988).
[16]L. M. Ziurys, Astrophys. J. Lett. **321**, L81 (1987).
[17]E. D. Tenenbaum, N. J. Woolf, and L. M. Ziurys, Astrophys. J. Lett. **666**, L29 (2007).
[18]S. T. Yamamura, K. Kawaguchi, and S. T. Ridgway, Astrophys. J. Lett. **528**, L33 (2000).
[19]K. M. Menten, F. Wyrowski, A. Belloche, R. Güsten, L. Dedes, and H. S. P. Müller, Astron. Astrophys. **525**, A77 (2011).
[20]W. M. Irvine, L. M. Ziurys, L. W. Avery, H. E. Matthews, and P. Friberg, Astrophys. Lett. Comm. **26**, 167 (1988).
[21]D. T. Halfen, D. J. Clouthier, and L. M. Ziurys, Astrophys. J. Lett. **677**, L101 (2008).
[22]K. Kawaguchi, Y. Kasai, S.-I. Ishikawa, M. Ohishi, N. Kaifu, and T. Amano, Astrophys. J. Lett. **420**, L95 (1994).
[23]M. Agúndez, J. Cernicharo, and M. Guélin, Astrophys. J. Lett. **662**, L91 (2007).
[24]P. F. Goldsmith and R. A. Linke, Astrophys. J. **245**, 482 (1981).
[25]L. E. B. Johansson, C. Andersson, J. Ellder, P. Friberg, A. Hjalmarson, B. Hoglund, W. M. Irvine, H. Olofsson, and G. A. Rydbeck, Astron. Astrophys. **130**, 227 (1984).
[26]Y. C. Minh, W. M. Irvine, and M. K. Brewer, Astron. Astrophys. **244**, 181 (1991).
[27]M. A. Frerking, R. A. Linke, and P. Thaddeus, Astrophys. J. Lett. **234**, L143 (1979).
[28]D. T. Halfen, L. M. Ziurys, S. Brünken, C. A. Gottlieb, M. C. McCarthy, and P. Thaddeus, Astrophys. J. Lett. **702**, L124 (2009).
[29]M. Agúndez, J. Cernicharo, J. R. Pardo, M. Guélin, and T. G. Phillips, Astron. Astrophys. **485**, L33 (2008).
[30]K. M. Lanzetta, in *Lyman Alpha Absorption: The Damped Systems,* in *Encyclopedia of Astronomy and Astrophysics*, edited by P. Murdin (Nature Publishing Group, Bristol, Philadelphia; Institute of Physics Pub, London, New York, 2001), Vol. II, pp. 1455–1457.
[31]H.-J. Werner, P. J. Knowles, G. Knizia, F. R. Manby, M. Schütz *et al.*, MOLPRO, version 2010.1, a package of *ab initio* programs, 2010, see http://www.molpro.net.
[32]P. J. Knowles, C. Hampel, and H.-J. Werner, J. Chem. Phys. **99**, 5219 (1993).
[33]P. J. Knowles, C. Hampel, and H.-J. Werner, J. Chem. Phys. **112**, 3106 (2000).
[34]K. Raghavachari, G. W. Trucks, J. A. Pople, and M. Head-Gordon, Chem. Phys. Lett. **157**, 479 (1989).
[35]P. J. Knowles and H.-J. Werner, Chem. Phys. Lett. **115**, 259 (1985).
[36]H.-J. Werner and P. J. Knowles, J. Chem. Phys. **82**, 5053 (1985).
[37]H.-J. Werner and P. J. Knowles, J. Chem. Phys. **89**, 5803 (1988).
[38]P. J. Knowles and H.-J. Werner, Chem. Phys. Lett. **145**, 514 (1988).
[39]H. J. Werner, T. B. Adler, and F. R. Manby, J. Chem. Phys. **126**, 164102 (2007).
[40]T. B. Adler, G. Knizia, and H.-J. Werner, J. Chem. Phys. **127**, 221106 (2007).
[41]G. Knizia, T. B. Adler, and H.-J. Werner, J. Chem. Phys. **130**, 054104 (2009).
[42]K. A. Peterson, T. B. Adler, and H-J. Werner, J. Chem. Phys. **128**, 084102 (2008).
[43]F. Weigend, Phys. Chem. Chem. Phys. **4**, 4285 (2002).
[44]C. Hättig, Phys. Chem. Chem. Phys. **7**, 59 (2005).
[45]W. Klopper, Mol. Phys. **99**, 481 (2001).
[46]T. H. Dunning, J. Chem. Phys. **90**, 1007 (1989).
[47]D. E. Woon and T. H. Dunning, Jr., J. Chem. Phys. **98**, 1358 (1993).
[48]R. A. Kendall, T. H. Dunning, Jr., and R. J. Harrison, J. Chem. Phys. **96**, 6796 (1992).
[49]D. E. Woon and T. H. Dunning, Jr., J. Chem. Phys. **103**, 4572 (1995).
[50]K. A. Peterson and T. H. Dunning, Jr., J. Chem. Phys. **117**, 10548 (2002).
[51]T. H. Dunning, Jr., K. A. Peterson, and A. K. Wilson, J. Chem. Phys. **114**, 9244 (2001).
[52]J. W. Cooley, Math. Comput. **15**, 363 (1961).

[53]M. Hochlaf, G. Chambaud, P. Rosmus, T. Andersen, and H. J. Werner, J. Chem. Phys. **110**, 11835 (1999).
[54]S. Ben Yaghlane, S. Lahmar, Z. Ben Lakhdar, and M. Hochlaf, J. Phys. B **38**, 3395 (2005).
[55]S. Ben Yaghlane and M. Hochlaf, J. Phys. B. **42**, 015101 (2009).
[56]H. Lefebvre-Brion and R. W. Field, *The Spectra and Dynamics of Diatomic Molecules* (Elsevier Academic, New York, 2004).
[57]A. Maatouk, A. Ben Houria, O. Yazidi, N. Jaidane, and M. Hochlaf, J. Chem. Phys. **133**, 144302 (2010).
[58]See supplementary material at http://dx.doi.org/10.1063/1.4730303 for the evolution of the off-diagonal spin-orbit integrals of PS (Figure S1). We give also the dominant electron configuration of PS, $PS^+$, and $PS^-$ electronic states at equilibrium and at large internuclear distances (Table S1).
[59]G. Herzberg, *Molecular Spectra and Molecular Structure: Spectra of Diatomic Molecules* (Van Nostrand, 1950).
[60]See http://webbook.nist.gov for the experimental molecular constants of $NO^+$ and $NS^+$ cations.
[61]L. E. Bullock and C. D. Hause, J. Mol. Spectrosc. **39**, 519 (1971).
[62]H. Ndome, M. Hochlaf, B. R. Lewis, A. N. Heays, S. T. Gibson, and H. Lefebvre-Brion, J. Chem. Phys. **129**, 164307 (2008).
[63]R. W. Field, O. Pirali, and D. W. Tokaryk, J. Chem. Phys. **124**, 081103 (2006).